Int. Journal of Refractory Metals and Hard Materials 56 (2016) 35–43

Contents lists available at ScienceDirect

Int. Journal of Refractory Metals and Hard Materials

journal homepage: www.elsevier.com/locate/IJRMHM

Microstructural evolution of mechanically alloyed Mo–Si–B–Zr–Y powders

Tao Yang, Xiping Guo *, Yucheng Luo

State Key Laboratory of Solidification Processing, Northwestern Polytechnical University, Xi'an 710072, China

ARTICLE INFO

Article history:
Received 28 October 2015
Received in revised form 26 November 2015
Accepted 30 November 2015
Available online 17 December 2015

Keywords:
Mechanical alloying
Molybdenum solid solution
Microstructure
Miedema model
Nanostructured material

ABSTRACT

Elemental powder mixtures with compositions of Mo–13.8Si, Mo–20B and Mo–12Si–10B–3Zr–0.3Y (at.%) were respectively milled in a high energy planetary ball mill at a speed of 500 rpm. Microstructural evolution of powder particles during milling processes was evaluated. The results show that B can hardly be dissolved into Mo under present milling conditions and the additions of B and Si both accelerate the refining rate of Mo crystallites. For Mo–12Si–10B–3Zr–0.3Y system, the morphology and internal structure of powder particles change significantly with milling time. After 40 h of milling, an almost strain-free super-saturated molybdenum solid solution with a grain size of about 6.5 nm forms. The grain refinement mechanism and dissolution kinetics of solute atoms are highlighted. Both thermodynamic calculation and experimental results reveal that for the present alloy composition it is more favorable to form solid solution than amorphous phase.

1. Introduction

Mo–Si–B based alloys located in the Moss (molybdenum solid solution), Mo_3Si and Mo_5SiB_2 (T2) three-phase region exhibit excellent oxidation resistance, outstanding high temperature mechanical properties and moderate room temperature fracture toughness and have great potential as ultrahigh temperature structural materials [1]. However, due to their extremely high melting temperatures, it is more reasonable to fabricate this kind of alloys by powder metallurgy. Mechanical alloying (MA) is a common powder processing technology, which has important effects on the following consolidation procedure. Firstly, energy stored in heavily deformed particles can act as driving force to reduce the sintering temperature [2]. Secondly, MA can be used to synthesize ultra-fine materials that can display super-plasticity even at a relatively low temperature and high strain rate providing the opportunity of thermo-mechanical processing of this kind of alloys [3–5]. Finally, MA is a promising method to fabricate Mo–Si–B alloys with a continuous α-Mo matrix, which can decrease the brittle-to-ductile transition temperature (BDTT) by about 150 °C [3,6,7]. A lot of researches revealed that alloying element Zr, which reacted with oxygen to form ZrO_2 or segregated to the grain boundaries, could increase both the strength and the plasticity of Mo–Si–B alloys by refining grains, forming dispersion particles and increasing grain boundary cohesion [8–11]. It is well known that Y_2O_3 can significantly reduce grain boundary mobility during sintering process and therefore stabilize the fine grain size produced by MA, which can increase the room temperature mechanical property of materials [8,12]. Besides, it has been proven that Y is also beneficial to the oxidation resistance of Mo–Si–B alloys [13]. Based on these considerations, an alloy with a nominal composition of Mo–12Si–10B–3Zr–0.3Y (hereafter all compositions are given in at.% unless otherwise stated) is designed. The present work focuses on the MA process of powders from the point of microstructural evolution to lay the foundation for the following consolidation procedure.

Krüger et al. [7] studied the MA behavior of Mo–8B mixed elemental powders and found that no significant concentration of B dissolved during the MA process. However, Abbasi et al. [14] found that the lattice constant of Mo showed a slight increase in the initial milling stage of Mo–12.5Si–25B elemental powder mixture, which was attributed to the dissolution of B into Mo. Obviously, there exists a discrepancy about the dissolution characteristic of B in Mo in these two researches. As a result, other two binary systems, Mo–13.8Si and Mo–20B, have been designed to study the dissolution characteristics of Si and B and their effects on the MA process.

The semi-empirical Miedema model is widely used to calculate the formation energies of solid solution and amorphous phase and successfully predicts the MA products [15,16]. Here, a thermodynamic analysis based on this method is also conducted to illuminate the experimental results.

2. Experimental procedures

Mo, Si, B (amorphous state), Zr and Y elemental powders with a purity of 99% or better were used as raw materials. MA was conducted in a high energy planetary ball mill using stainless steel vials and balls under protective atmosphere. The milling speed and ball-to-powder

* Corresponding author.
E-mail address: xpguo@nwpu.edu.cn (X. Guo).

http://dx.doi.org/10.1016/j.ijrmhm.2015.11.012
0263-4368/

ratio (BPR) were 500 rpm and 15:1 respectively. The milling time was 1, 2, 5, 10, 15, 20, 30 and 40 h respectively. One quinary and two binary systems with compositions of Mo–12Si–10B–3Zr–0.3Y, Mo–20B and Mo–13.8Si were milled respectively. Besides, pure Mo was also milled under the same experimental conditions as reference.

The phase constituents of powders were characterized by X-ray diffractometer (Panalytical X'Pert Pro) with a Cu target ($\lambda_{K\alpha1} = 0.154$ nm) operating at 40 kV and a step size of 0.0167°. Simultaneously, X-ray diffraction (XRD) results were also used to calculate the grain size, microstrain and lattice constant of Moss based on the Williamson–Hall [17] and Cohen methods [18], respectively. The instrumental line broadening was determined using a standard Si sample.

The microstructural evolution of powder particles was examined using a scanning electron microscope (SEM, Tescan MIRA3) and the chemical compositions of Moss were determined by energy-dispersive X-ray spectrum analyzer (EDS, Inca X-sight). To observe their internal structures, the powder particles were mounted by epoxy resin, ground using a series of abrasive papers and then polished by Al_2O_3 abrasive paste. The microstructure of powder particles was also observed using a transmission electron microscopy (TEM, Tecnai G^2 F30). Image-Pro Plus (IPP) was applied for the statistical analysis of the Moss grain size from the TEM data to verify the calculation results of Williamson–Hall method.

3. Results and discussion

3.1. MA behaviors of Mo–20B and Mo–13.8Si particles

As mentioned above, some previous studies [7,14] showed a discrepancy about the dissolution of B in Mo. Thus, this section aims at illuminating the dissolution characteristic of B in Mo under present experimental conditions to get a better understanding of the MA mechanism of Mo–12Si–10B–3Zr–0.3Y system. Fig. 1 shows the XRD patterns of the original Mo and Mo, Mo–13.8Si and Mo–20B milled for 40 h. The Mo peaks in the XRD patterns of unmilled Mo–13.8Si and Mo–20B powders are quite consistent with those in pure Mo. Therefore, the XRD patterns of unmilled Mo–13.8Si and Mo–20B powders are not listed for clarity. It can be seen that for pure Mo system after 40 h of milling the Mo peak position does not change significantly and still coincides with the standard data of Mo (dashed line). EDS analysis shows that after 40 h of milling the Fe content in Moss is under 1 at.%, less than the critical value (2.5 at.%) proposed by Krüger et al. [7], and

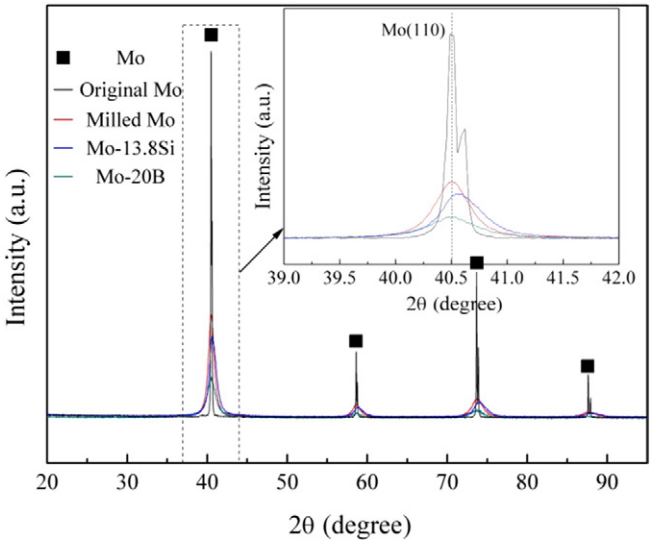

Fig. 1. XRD patterns of the original Mo and Mo, Mo–13.8Si and Mo–20B milled for 40 h. The inset is the enlarged view of Mo(110) peaks. The dashed line shows the standard position of Mo (110) peak (PDF 89-4896).

therefore, has a negligible effect on the lattice constant of Moss, which is consistent with the XRD result. After 40 h of milling, the Mo peak position in Mo–13.8Si shifts to a higher 2θ angle significantly, which means an extensive dissolution of Si into Mo. While for Mo–20B after 40 h of milling the Mo peak position still shows a good agreement with that of pure Mo system, which is also true for lattice constant shown in Table 1, indicating no significant concentration of B dissolved during this MA process.

Fig. 2 shows the cross-sectional back-scattered-electron (BSE) images of powder particles with the compositions of Mo–13.8Si and Mo–20B milled for 5 h or 40 h. For the Mo–13.8Si system after 5 h of milling Si particles are dispersed among Mo lamellas (Fig. 2(a)). With increasing milling time to 40 h, uniform Moss forms extensively and there remain few discernable Si particles (Fig. 2(b)). When it comes to Mo–B system, even after 40 h of milling, there still are lots of B particles dispersing in the Mo matrix, as shown by the arrows in Fig 2(c).

From what has been discussed above, it can be concluded that under the present MA conditions it is hard for B to dissolve into Mo lattice, which is consistent with the conclusion proposed by Krüger et al. [7].

It is also shown in Fig. 1 that after 40 h of milling the intensity of diffraction peaks decreases and the full widths at half maximum (FWHMs) of Mo peaks are broadened as a result of grain size refinement and/or accumulation of the lattice microstrain. Besides, with the additions of Si and B brittle particles, the diffraction peaks show lower intensity and broader FWHMs. Table 1 lists the grain size and microstrain of Mo or Moss in the systems of pure Mo, Mo–13.8Si and Mo–20B after 40 h of milling. It can be found that the additions of Si and B particles both accelerate the refining progress of Mo crystallites. While due to the different dissolution characteristics of these two kinds of particles, the corresponding refining mechanisms are different. Sturm et al. [19] revealed that with increase in its Si concentration, the room temperature ductility and fracture toughness of Moss dropped precipitously. Therefore, the accelerated refinement behavior of Mo crystallites by Si particles can be attributed to the increasing fragmentation tendency of Mo with the continuous dissolution of Si atoms, similar to the MA behavior of Cu–Nb powders studied by Lei et al. [20]. While the ultrafine B particles just act like countless "micro-milling balls" to compact, micro-frict and micro-cut the Mo powders to enhance their milling intensity [21].

3.2. MA behavior of Mo–12Si-10B–3Zr–0.3Y particles

3.2.1. Morphological and internal structural evolution of powder particles

Fig. 3 shows the secondary-electron (SE) images and corresponding cross-sectional BSE images of powder particles after different milling time. Generally, the particle morphology and internal structure change with the progress of mechanical alloying significantly under the actions of deformation, cold welding and fracturing mechanisms [22]. For the present system, after 2 h of milling, the powder particles are deformed intensively and lose their original morphological characteristics. There appear some large and irregular composite particles (Fig. 3(a)). Under the action of milling media, the ductile components are flattened by a micro-forging process, while the brittle ones get fragmented. The resulting particles show fresh surfaces. As a consequence, they are easily cold welded together to form composite particles with a lamellar structure, where the brittle particles are embedded in the ductile lamellas or dispersed in the interlamellar spaces (Fig. 3(b)). With increasing milling time to 5 h, as a result of repeated plastic deformation, the powder

Table 1
Lattice constant, grain size and microstrain of Mo or Moss in different milling systems after 40 h of milling.

Milling system	Lattice constant (nm)	Grain size (nm)	Microstrain (%)
Mo	0.31472 ± 0.00004	38.8 ± 3.5	0.716 ± 0.021
Mo–13.8Si	0.31383 ± 0.00007	27.9 ± 2.4	0.769 ± 0.028
Mo–20B	0.31472 ± 0.00008	13.0 ± 0.8	0.648 ± 0.045